Electronic Supplementary Material (ESI) for Physical Chemistry Chemical Physics.

Lysozyme Adsorption at a Silica Surface Using Simulation and Experiment: Effects of pH on Protein Layer Structure

Karina Kubiak-Ossowska[†], Monika Ćwięka[$], Agnieszka Kaczyńska[++], Barbara Jachimska[$] and Paul A. Mulheran[†]*

[†]Department of Chemical and Process Engineering, University of Strathclyde, James Weir Building, 75 Montrose Street, Glasgow G1 1XJ, United Kingdom

[$] J. Haber Institute of Catalysis and Surface Chemistry, Polish Academy of Science (PAS), Niezapominajek 8, 30-239 Cracow, Poland

[++]*Jagiellonian University, Faculty of Chemistry, Ingardena 3, 30-060 Cracow, Poland*

SUPLEMENTARY MATERIALS

I. MD PROTOCOL DETAILS

All simulations were performed with the NAMD 2.6[1] package using the ChARMM27 force-field, and analyzed using VMD.[2] 1iee.pdb[3] with all four disulphide bridges kept was used as the starting HEWL structure. We prepared twelve simulation systems and ran 100ns adsorption trajectories for each of them. Since the net charge of the protein was +8e, the protein was initially neutralized by adding NaCl salt at an ionic strength $I=2x10^{-2}$ M, then the surface was added to the systems and finally the rectangular water box (TIP3P model) was introduced. Water box dimensions were 86Å x 89Å (SiO_2 surface dimensions) x 100 Å (water/protein space) with the protein located in the center of the box. In total we have obtained twelve adsorption trajectories at the silica surface. All simulations were run in NVT ensemble with the temperature of 300K.

For the silica surface model, similarly to our recent work[4,5] a $(10\bar{1})$ slab of α-cristabolite with dimensions 86 Å x 89 Å x 13 Å was used following Patwardhan *et al.*[6] The SiO_2 slab model (Fig. S1) is neutral and stoichiometric, but the slab has been cut from a bulk crystal in such a way as to leave siloxide groups ($\equiv SiO^-$) at the top of the slab and under-coordinated Si species at the bottom; the slab then has an intrinsic dipole moment across it since we model the material as ions fixed in space. The 3D periodicity of the simulation cell thus creates an electric field across the water/peptide space, mimicking the electric field above a single negatively charged silica surface comprising siloxide species[6] (Fig. S1). In the case of $pSiO_2$ shown in Fig. S1b, the silica slabs are inverted so that these simulations can be considered as alternative trajectories for SiO_2 adsorption. Note that in experiments at pH7, the siloxide groups of the SiO_2 surface are exposed to the solvent, so that our SiO_2 surface, rather than the $pSiO_2$, is actually observed. In adsorption simulations the polarizing effect driving ions to the oppositely charged surface slab is observed, e.g. sodium ions migrate toward the siloxide-rich surface (lower on Fig. S1a and upper on Fig. S1b), while chloride

ions migrate toward the Si+-rich surface (upper on Fig. S1a and lower on Fig. S1b). We note that the Ewald summation has metallic boundary conditions with no jump in electrostatic potential across the box, so the magnitude of the electric field in the middle of the simulation box depends on the slab dipole moment and the overall box height.[7] We measure the electric field in the empty SiO_2 box to be 0.2 V/Å, corresponding to 0.16 charged silanol groups nm^{-2}, which is comparable to estimates for large silica nanoparticles at pH 7.[6] Thus, the surface models present realistic charge density as well as differing surface chemistry. Of course, in the presence of an ionic solution, the electric field is screened with Debye lengths of 30.4 for 0.05 M.

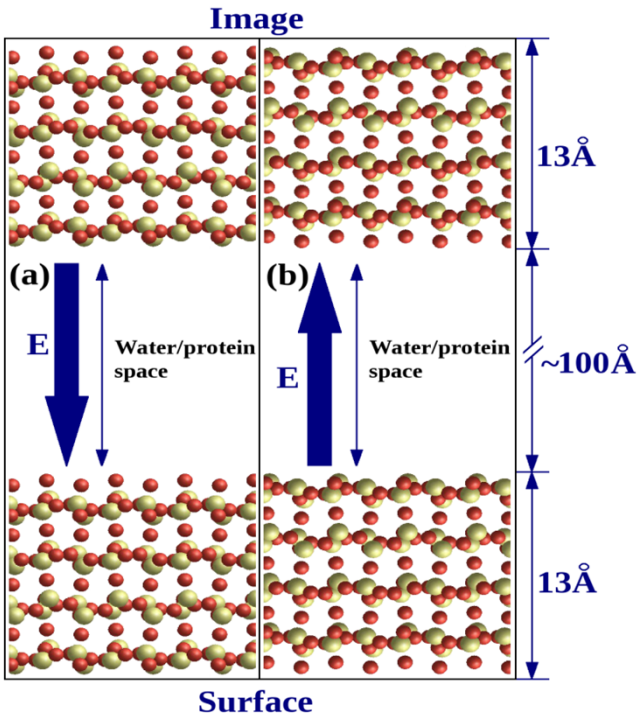

Figure S1. Illustration of the simulation cells and crystal structures used in this study for SiO_2 and $pSiO_2$ surface; silicon is yellow and oxygen is red. (a) The SiO_2 surface: the alpha-cristobalite $(10\bar{1})$ surface is cut so that the upper surface is terminated with under-coordinated oxygen, inducing an electric field E across the water/peptide space due to the dipole moment of the crystal slab. (b) The $pSiO_2$ surface: the slab flipped vertically.

In order to simulate the silica surfaces we have parameterized the force-field following the work of Patwardhan *et al.*[6] by adjusting the parameters of the CHARMM27 force-field. The parameters we use are summarized in Table S1. Note that siloxide oxygen ions have the same charge as the bulk silica oxygen ions. The Si-O bonds and Si-O-Si bond angles were not included in the parameterization, since surface silicon and oxygen were fixed in all stages of our MD simulations. Since both SiO_2 and $pSiO_2$ were initially placed in six various orientations in respect to the protein we have obtained twelve 100 ns trajectories denoted as SiO_2V1, …, SiO_2V6 and $pSiO_2$V1, … , $pSiO_2$V6.

Table S1. Charmm27 force-field parameters used in variants of the α-cristabolite $(10\bar{1})$ slab.

Charges		
Atom	Charge (e)	
Bulk silica	+1.10[a]	
Bulk oxygen	-0.55[a]	
Van der Waals		
Atom	ε_0 (kcal/mol)	½ R_0 (Å)
Bulk silicon	-0.50[a]	2.00[a]
Bulk oxygen	-0.25[a]	1.75[a]

Various surface locations were obtained by changing the surface plane and location in respect to the protein, while the distance was always 28 Å. In trajectories denoted as V1 the surface was located in the (*x,y)* plane, below the N,C-terminal face, while in V2 trajectories the surface was located above the protein. Trajectories V3 and V4 were obtained by putting the surface in the (*y,z)* plane close to the end nearest to the N,C-terminal face (V3) or close to the opposite protein end nearby the minor adsorption site (V4). Finally, in trajectories V5 and V6 the surface lies in the (*x,z)* plane on both sides of the protein. The protein – surface initial orientations are shown in Figure S2.

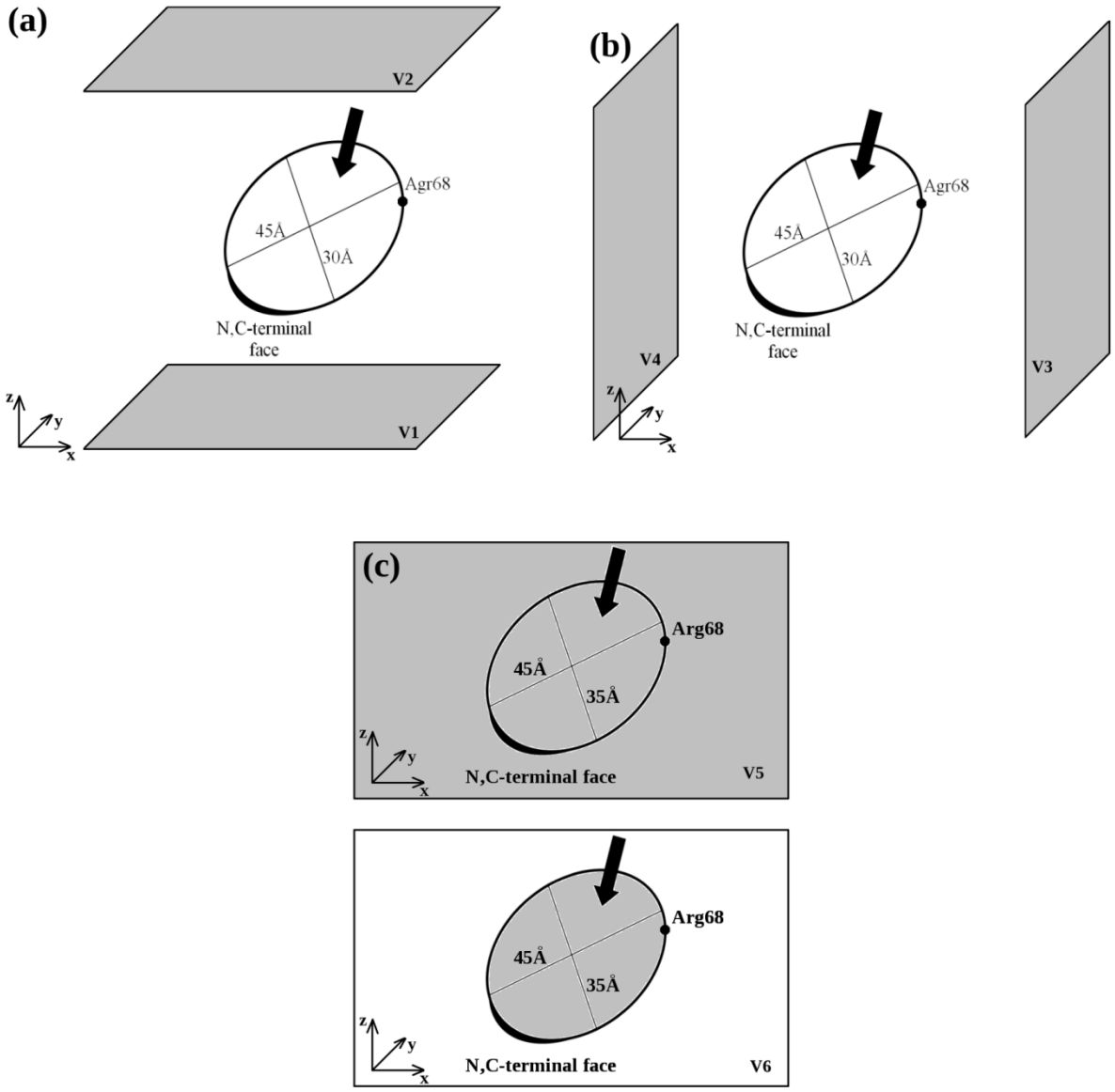

Figure S2. Schematic representation of the initial HEWL – surface arrangements: (a) Orientation in trajectories denoted as V1 and V2, (b) Orientation in trajectories denoted as V3 and V4, (c) Orientation in trajectories denoted as V5 and V6. The protein is shown as an ellipsoid with its two major axes; the N,C-terminal face and the minor adsorption site (Arg68) are indicated. The arrow points to the active site location.

The systems were subject to 1000 steps of water minimization only followed by 100ps water equilibration at the target temperature 300K, 10,000 steps of water and protein minimization, 30ps heating to 300K and equilibration of the entire system for 270ps in the constant temperature. The production MD simulations were pursued for 100ns at 300K in the NVT ensemble. The integration step was 2 fs, the SHAKE algorithm and PBC were used. The cut-off distance for van der Waals interactions was 12 Å, and the smooth particle mesh Ewald (SPME) summation,[8,9] was used for the Coulomb interactions. For ionizable residues, the most probable charge states at pH 7 were chosen. No additional restrictions on momentum in the simulations were used. Such a protocol has been already used[4,5,10-14] and it accuracy has been already discussed.[11]

II. DETAILED DESCRIPTION OF THE EXEMPLAR TRAJECTORIES

1. "Between" Orientation exemplar trajectory SiO_2V1

In the typical, exemplar trajectory ($V1SiO_2$.avi) HEWL rotates to expose N,C terminal face to the surface and the C-terminal part with Arg128 detaches from the protein surface during the equilibration trajectory what enhances Arg128 – surface interactions and allows this residue to adsorb as a first anchor (0.28 ns of the production trajectory). Initially Arg128 side chain is perpendicular to the surface, but a strong attraction between the surface and other charged protein side chains results in changing the geometry of the side chain which bends and achieves a parallel orientation in respect to the surface (0.56 ns); in such orientation the arginine – surface interactions are stronger, but it requires reorganization of the surface water layer. Then other charged NC-terminal face residues adsorb: Arg5 (2 ns), Arg125 (2.68 ns) and Lys1 (2.8 ns) with initially perpendicular side chains. The strong attraction results in protein flattening on the surface, as the result most of the anchor residues side chains switch

their orientation to the parallel (~6 ns). Before charged residues from α-helix A, namely Lys13 (7.76 ns) and Arg14 (9 ns) adsorb, some conformational changes in the N-terminal part and the loop connecting this helix with the next one (residues #17 - #24) are required. In this exemplar trajectory HEWL is adsorbed within first 3 ns of the trajectory and the list of the most important, anchoring residues consist: Arg128, Arg5, Arg125, Lys1, Lys13 and Arg14 (Tab. S2, Fig. 2). Other residues (Tab. S2) establish contact with the surface not because of their high propensity to the surface but because of the structural reasons; residues Gly126, Cys6, Cys127, Glu7, Tyr20 and Val2 are on the protein part facing the surface and frequently interact with the surface using their backbone hydrogens. At the end on the trajectory Lys116 from unfolded α-helix D adsorbs (98.92 ns), what may suggest that the stage after 100 ns may not be a final one. Note that the similar conclusion was made in the case of HEWL adsorption on mica.[15]

Protein conformational changes are observed during the entire trajectory. Initially changes in the N and C-terminal ends structure (detachment from the protein surface) resulting in Arg128 and Arg125 (C-ter), and Arg5 and Lys1 (N-ter) adsorption are visible. Then slower changes in loops connecting helices, resulting in Lys13 and Arg14 adsorption (α-helix A) and C-terminal α-helix 3_{10} unfolding, due to interactions with the surface are observed. Finally, slow changes such as unfolding of internal α-helices (namely helix B and D) are detected.

2. "Side-on" Orientation exemplar trajectory $pSiO_2V5$

The adsorption mechanism resulting in HEWL "side-on" orientation on the surface is described in the details for the exemplar trajectory $pSiO_2V5$; the mechanism is common for all trajectories.

As is shown in Figure S3, initially HEWL N,C-terminal face is exposed to the uncoordinated Si+ species (image) rather than to the siloxane-rich groups from the surface. The closest residue to the surface is Arg73 located on the side of the protein, HEWL dipole moment is oriented out of the surface with the angle 45^0. The same angle is between protein long axis and the surface. Similarly to "between" adsorption, the protein – surface interactions are visible during the heating and equilibration part of the trajectory. Initially protein dipole moment orients towards the surface then protein starts to rotate as a whole body to expose N,C-terminal face, simultaneously protein translates towards the surface. At the end of 300ps heating and equilibration period HEWL is 16.5 Å away from the surface, the dipole moment is oriented towards the surface (45^0) and the angle between protein long axis and the surface is 20^0. The rotation and attraction to the surface is continued during the production trajectory.

Because of strong attraction of side residues (Arg73 and Arg14) there is no enough time to rotate and expose N,C-terminal face, what results in Arg14 adsorption in 1.32 ns, the side chain is perpendicular to the surface. Attraction to the surface is continued and at 1.6 ns Arg73 adsorbs, also with perpendicular side chain. At 1.64 ns Asn77 adsorbs and from this moment HEWL is adsorbed in "side-on" orientation. In the meantime also other, minor residues establish contacts with the surface (see Tab.S2). The next important moment is seen at 2.76ns when Arg73 side chain changes its orientation to the parallel in respect to the surface. Attraction and flattening on the surface is continued, other anchors located at the protein side adsorb: Asn93 (2.92 ns), Ser86 (3.28 ns), Ser85 (3.48 ns). Lys1 adsorbs at 4.08 ns, for Arg128 adsorption a conformational change of C-ter is required and this residue adsorbs at 5.76 ns. Conformational changes in protein long loop (residues #61 - #78) results in Arg68 adsorption at 17.32 ns, simultaneous changes in α-helix A region result in Arg 5 (18.68 ns) adsorption. At this stage a meta-stable state is reached: protein long axis angle in respect to the surface is 0^0, the dipole moment is printed towards the surface with the angle

fluctuating between 60^0 – 80^0 and the long loop #61 - #78 is detached from the protein surface. Late adsorption of Lys13 and Arg21 (87.88 ns) is possible due to α-helix A reorientation.

The first substantial conformational changes are alterations in the long loop #61-#78 regions which result in Arg78 and Asn77 adsorption and observed a bit later Arg68 adsorption. Changes in N,C-terminal face result in Lys1 and Arg128 adsorption.

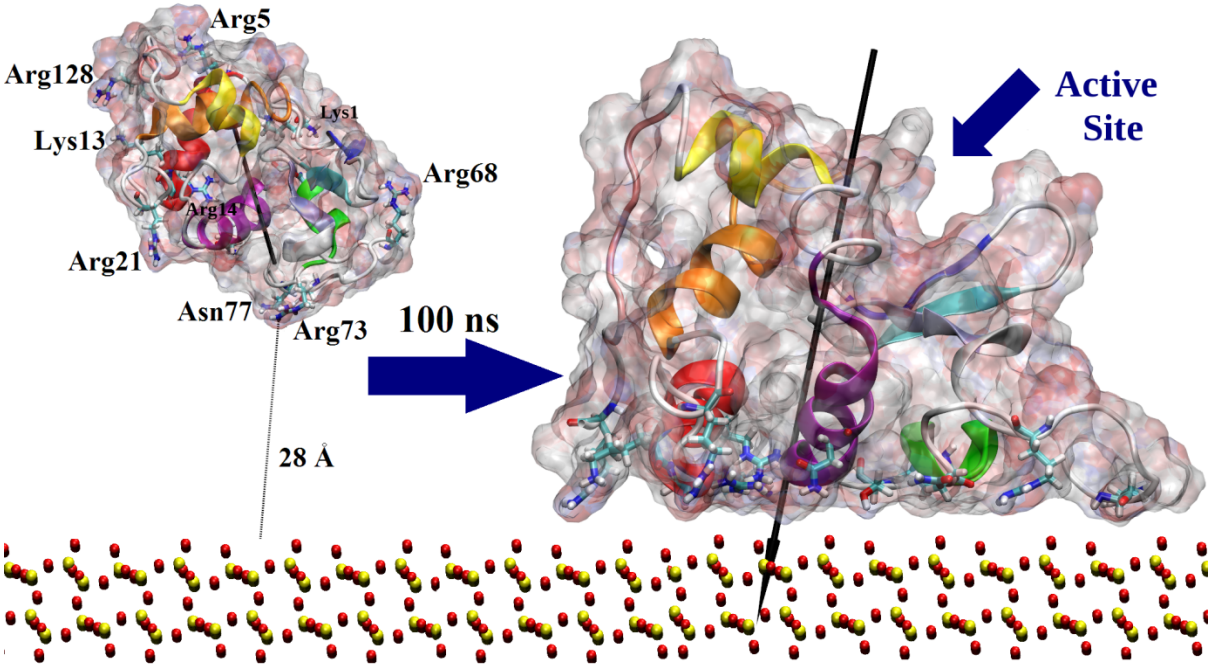

Figure S3. Initial (left) and final (right) adsorption stage for the exemplar "side-on" trajectory ($pSiO_2V1$). The coloring scheme is the same as in Fig. 2.

Combining with other trajectories resulting in "side-on" adsorption we conclude that in some cases when in the initial structure the side-located charged residues (Arg73 and Arg14) are exposed towards the surface instead of N,C-terminal the attraction is so strong that protein is not able to rotate and expose the N,C-terminal face and do is trapped in "side-on" orientation on the surface. Eventual adsorption of the N,C-terminal residues cannot

change HEWL orientation on the surface because the energetic barriers are too high to cross during 100 ns trajectory.

The list of the most important residues for "side-on" adsorption (in order of importance) seems to be as follow: Arg14, Arg114, Arg73, Arg45, Aer86, Ser85, Arg68, Arg128, Lys1, Arg125, Arg5, Asn77, Asn93, Lys13, Arg21, Ser81. It is worth to note that in the case of "side-on" adsorption the role main anchors can be played also by not charges (but polar) residues as serine and asparagine, while in "between" adsorption they serve only as minor anchors.

The structural changes upon "side-on" adsorption seem to be slightly more serious than in the case of the "between" orientation (for details see below), nevertheless adsorbed protein can maintain its activity.

3. Structural Changes upon Adsorption

Structural changes in all obtained trajectories can be analyzed basing on RMSD and RMSF plots shown in Fig. S4. The range of conformational changes strongly depends on the trajectory. As is indicated in Tab. S2 and visualized in Fig. S4 the list of secondary structures which can unfold consists: both α-helices 3_{10}, α-helix D and all three β-sheets. Structures which unfold only partially include: α-helices A and B and both α-helices 3_{10}. Among structures which conformation is only slightly affected by the adsorption are: all long α-helices (A, B, C and D) and C-terminal α-helix 3_{10}. Careful analysis of Tab. S2 and Fig. S4 indicate that usually C-terminal α-helix 3_{10}, and α-helix D unfold while the most stable structures are α-helix C and middle α-helix 3_{10}. The general trend differentiating "side-on" and "between" final conformations is not observed, nevertheless it seems that in the case of "side-on" adsorption the conformational changes are more serious than in the case of "between" orientation, particularly in the long loop region, which is close to the active site,

therefore HEWL activity can be potentially affected by “side-on” adsorption. To confirm (or reject) this hypothesis a larger sample of trajectories is be required.

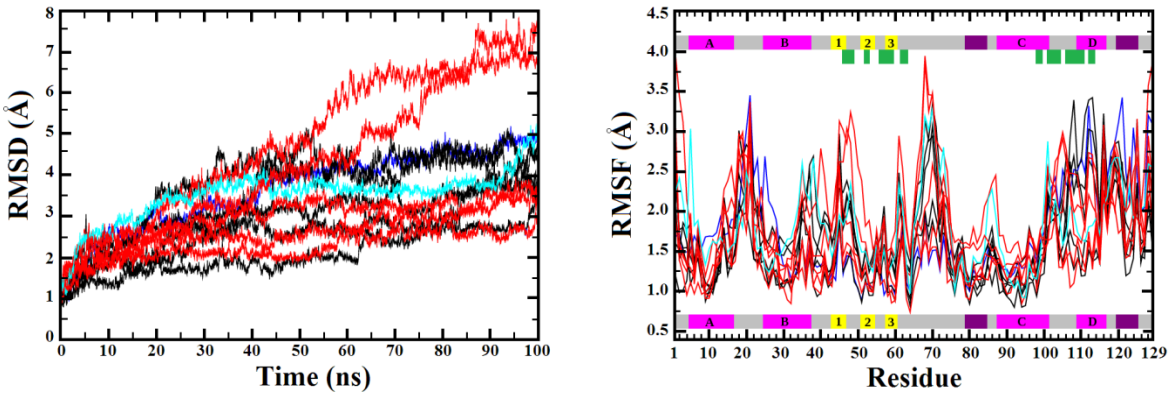

Figure S4. RMSD (left) and RMSF (right) plots calculated with respect to the initial HEWL structure during: SiO_2 surface adsorption trajectories (black), $pSiO_2$ surface adsorption trajectories (red), plots for exemplar trajectories are indicated in blue (SiO_2V1) and cyan ($pSiO_2$V5). The color ribbon at the RMSF indicates secondary structure of initial HEWL: loops are shown in gray, β structures in yellow, α-helices in pink and α-helices 3_{10} in purple. For clarity β bridges and turns in loops regions are not shown main secondary structure elements are annotated. Green ribbon indicates location of the active site. The preparation period (minimization, heating and equilibration) is omitted.

The final RMSD values (Tab. S.2, Fig. S4) vary from 2.83 to 7.50 Å with the most frequent value 3.0–3.5 Å and the average value of 4.4 Å. Two trajectories with the highest RMSD are: SiO_2V4 and $pSiO_2$V6 (see also Tab S2). In both cases high RMSD values are mainly caused by considerable structural change of the long loop region which detaches from the protein surface to allow its arginines to adsorb. In turn it seems to accelerate other conformational changes and secondary structure alterations (see Tab S2 for the details). Usually they are also responsible for the highest RMSF values. In general relatively high RMSD values observed for the average trajectory, without visual analysis would suggest that

HEWL structural changes upon adsorption on SiO_2 surface are rather substantial, nevertheless overlaps of protein initial and final structure shown in Figure S3 indicate that the biggest changes come from loops and terminal regions (N,C-terminal face), while the overall shape, and the geometry of the active site is maintained relatively well. Having the fact that even small geometrical protein changes may potentially affect the activity of the enzyme we conclude HEWL activity may be affected by the adsorption, at least in some cases (SiO_2V4 and pSiO_2V6, what is equial to 1/6 trajectories). Nevertheless, more advanced analysis on HEWL activity, required to confirm or contradict the above thesis is beyond the scope of presented work. On the other side, relatively large RMSD values can reflect experimental observation that HEWL adopts more flexible conformation on the silica surface.[16] Therefore, we conclude the substantial HEWL unfolding on SiO_2 surface appears accidentally, in 1/6 of the trajectories (namely SiO_2V4 and pSiO_2V6). In all trajectories the active site is exposed to the solute so the protein likely maintains its activity or the activity can be relatively easily (due to internal HEWL flexibility) restored.

It is worth to mention that in our previous studies on HEWL adsorption at the mica surface model[10-15] we also observed substantial structural changes in N,C-terminal and loop regions. In current work, strong electrostatic attraction to the SiO_2 surface results in substantial HEWL flattening on SiO_2 which causes unfolding of some secondary structures elements. However, HEWL is far away from the unfolded state and we anticipate that structural changes upon adsorption on SiO_2 surface may be reversible.

III. DETAILED ADSORPTION RESULTS FOR ALL TRAJECTORIES

Table S2. The summary of MD results for all adsorption trajectories (Tr) studied. The angle (a) between protein long axis and the surface and in brackets the angle between protein dipole

moment and the surface is given in deg. The final HEWL orientation on the SiO_2 surface (O) can be B for “between” or S for “side-on” orientation. The next column (Anchors) lists anchoring residues and the time of adsorption in ns is given in brackets while the following column (Other Residues) lists any other residues which establish close contact with the surface, the time is also given in ns. The next column describes structural changes observed in the 100 ns protein structure in reference to the initial structure. The last three columns give the protein (stable) adsorption time in ns (column T), the RMSD value in Å calculated in respect to the initial structure (column R) and specify if the protein is likely to be active (Y) or not (N) (column A).

Tr	a	O	Anchors	Other Residues	Structural changes	T	R	A
V1	45 (80)	B	Arg128 (0.28), Arg5 (2), Arg125 (2.68), Lys1 (2.8), Lys13 (7.76), Arg14 (9), Lys116 (98.92)	Gly126 (1.16), Cys6 (2.68), Cys127 (2.68), Glu7 (2.68), Tyr20 (50), Val2 (58.8)	α-helix 3_{10} (#120-125) and α-helix D: unfolded, α-helix B: partially unfolded	2.7	4.92	Y
V2	45 (80)	B	Arg128 (0.6), Arg125 (1.88), Arg5 (3.28), Lys1 (6.04), Lys33 (11.44), Arg114 (12.48), Arg112 (14.4), Lys116 (55.44)	Gly126 (1.76), Val2 (11.44), Asn113 (15.28), Asn37 (45.12)	α-helix 3_{10} (#120-125) and α-helix D: unfolded, α-helix B: affected	3.3	3.55	Y
V3	45 (45)	B	Lys1 (1.68), Ser86 (1.68), Arg128 (3.04), Arg5 (4.88), Arg125 (11.6), Arg45 (66.52), Arg68 (79.2)	Gln41 (1.72), Val2 (2.12), Glu7 (3.08), Cys6 (12), Cys127 (12), Asn39 (17.44), Phe38 (17.64), Ser85 (78.8)	β1 and β3: unfolded, α-helix 3_{10} (#120-125) and α-helix D: unfolded	3.1	4.43	Y
V4	35 (80)	B	Lys1 (1), Arg128 (2.88), Arg5 (3.64), Arg125 (4.44)	Val2 (2.25), Glu7 (4.04), Ser86 (6.8), Cys6 (12.8), Cys127 (12.8)	α-helix 3_{10} (#120-125): unfolded	3.7	3.28	Y
V5	45 (60)	B	Arg128 (eq,260ps), Arg125 (0.04), Arg5 (0.68), Lys1 (4), Lys33 (36.28), Lys116	Gly126 (0.6), Cys127 (0.88), Phe34 (37), Asn37 (41.64),	α-helix 3_{10} (#120-125) and α-helix C: affected	0.7	3.93	Y

			(43.08)	Gln41(49.2),				
V6	60 (80)	B	Arg128 (0.2), Arg125 (0.4), Arg5 (0.6), Lys1 (1.4), Arg114 (6.8), Lys33 (6.8), Arg112 (16.12), Arg45 (58.84)	Gly126 (0.36), Val2 (5.92), Asn113 (15.72), Trp111 (56.8)	β1: unfolded, α-helix 3_{10} (#120-125)and α-helix D: unfolded, α-helix B: affected	0.6	4.55	Y
pV1	45 (80)	B	Lys1 (1.52), Arg114 (1.8), Lys116 (2.12), Arg125 (2.2), Lys1 (2.4), Lys33 (2.48), Arg5 (2.48), Arg128 (2.52), Arg112 (5.12)	Asn37 (2.56), Gly126 (2.56), Phe34 (2.56), Asn113 (4.88), Trp123 (4.96)	α- helix D: unfolded, α-helix 3_{10} (#120-125):partially unfolded	2.2	3.35	Y
pV2	0 (80)	S	Arg114 (1.36), Arg45 (1.88), Arg125 (1.88), Lys1 (1.92), Lys116 (3.56), Arg5 (7.16), Arg128 (58.56)	Asn37 (2.12), Thr47 (2.88), Phe34 (4.72), Val2 (5.64), Trp123(26.73)	α-helix 3_{10} (#120-125): unfolded, α-helix D: affected	1.9	2.83	Y
pV3	60 (80)	B	Arg128 (0.16), Arg125 (1.68), Arg5 (10.12), Lys1 (48.68), Lys116 (81.8), Arg114 (91.68), Lys33 (94.4)	Gly126 (0.72), Cys6 (11.92), Trp123 (91.16), Val2 (99.72)	α-helix 3_{10} (#120-125): unfolded, α- helix D: affected	10.2	3.32	Y
pV4	45 (60)	B	Arg128 (eq,285ps), Arg125(0.32), Arg14 (6.4), Lys1 (15.56), Arg21 (39.76), Asn19 (61.12), Lys116 (69.92), Arg112 (71.08),	Gly126 (0.4), Glu121 (67.92), Tyr23 (71.08), Tyr20 (86.8)	β1, β2 and β3: unfolded, α-helix D: unfolded, α-helix 3_{10} (#79-84), α-helix A and B: partially	6.4	6.31	N

			Arg73 (99.36)		unfolded, α-helix C and α-helix 3_{10} (#120-125): affected			
pV5	10 (60)	S	Arg14 (1.32), Arg73 (1.6), Asn77 (1.64), Asn93 (2.92), Ser86 (3.28), Ser85 (3.48), Lys1 (4.08) Arg128(5.76), Arg68 (17.32), Arg5 (18.68), Lys13 (87.88), Arg21 (87.88)	His15(1.76), Thr89 (1.76), Pro79 (2.36), Ile78 (2.92), Asp87 (3.44), Ala82 (4.08), Pro70 (16.88), Thr69 (79)	α-helix 3_{10} (#79-84):unfolded, α-helix A: affected	1.7	4.89	Y
pV6	0 (86)	S	Arg14 (1), Ser85 (1.08), Ser86 (1.08), Arg68 (1.72), Arg128 (3.08), Lys1 (3.24), Arg125 (46.24), Ser81 (71.12), Arg5 (83.88)	Ala8 (79.12), Pro79 (71.12)	β1, β2 and β3: unfolded, α-helix 3_{10} (#79-84): unfolded	1.1	7.50	N

IV. STRUCTURE OVERLAPS

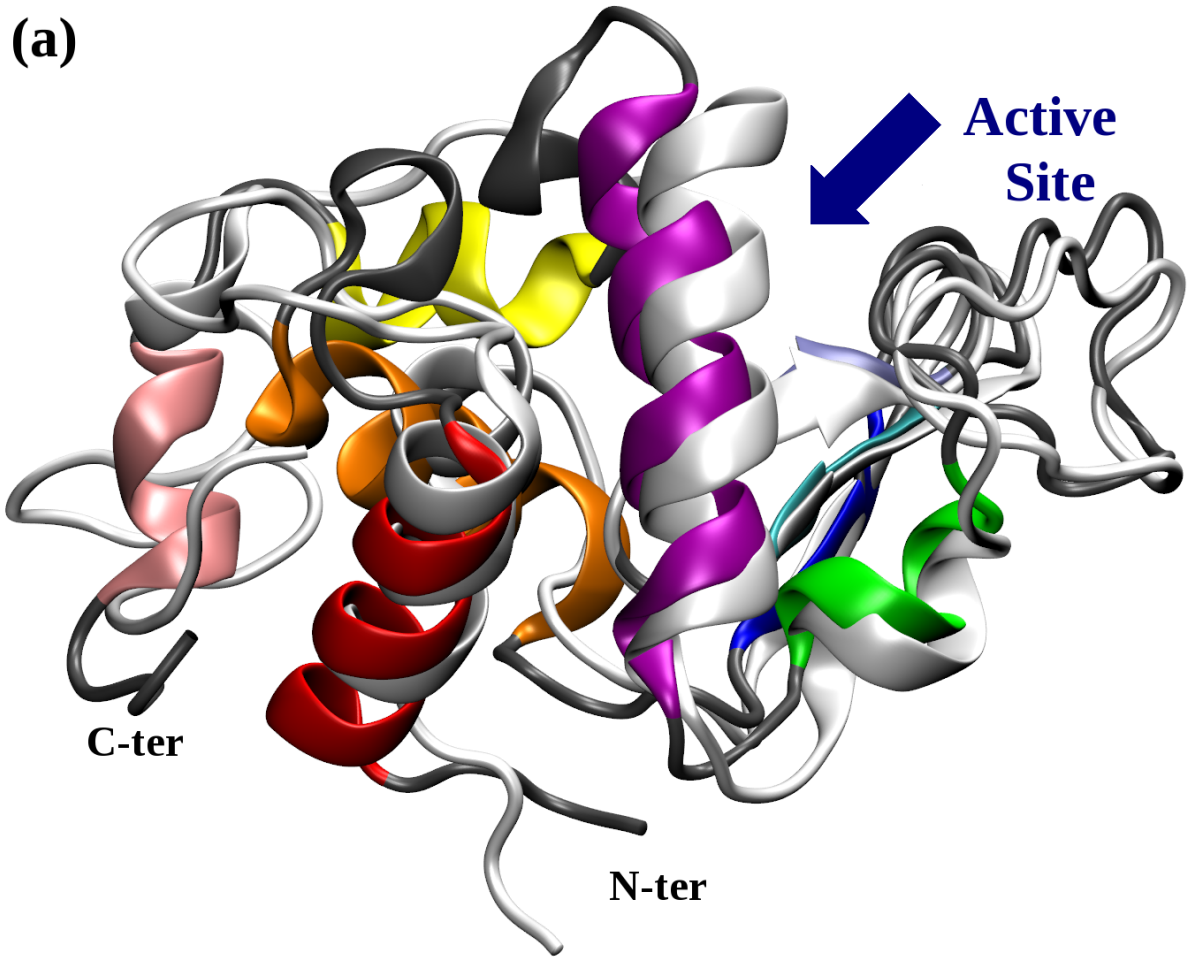

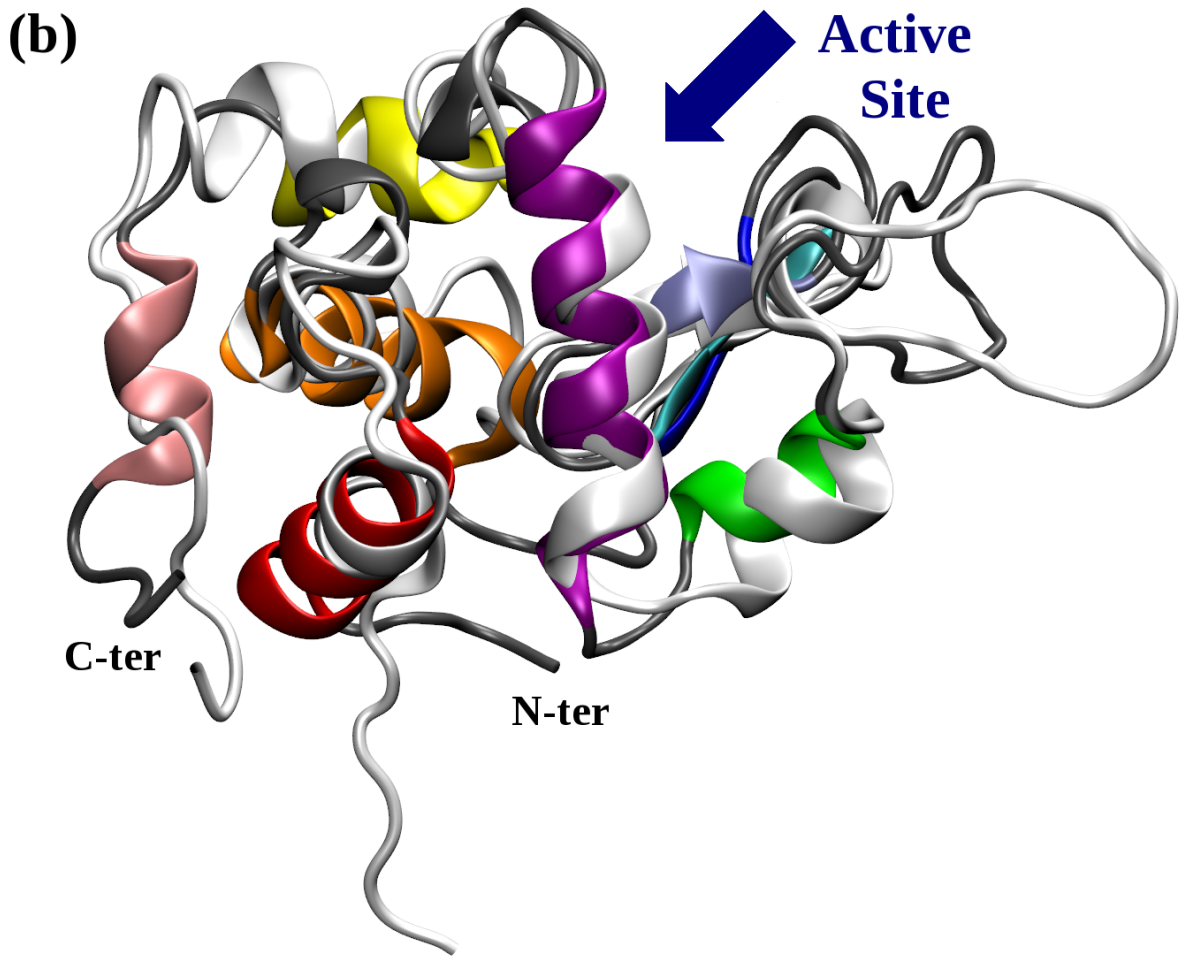

Figure S5. Overlap of the initial and final structure of HEWL obtained for representative trajectories: (a) SiO_2V1 and (b) pSiO_2V5. Protein secondary structure is shown as a cartoon colored by structure (initial structure) and in white (100 ns structure). Protein ends are annotated.

V. MOVIES

SiO_2V1.avi – a movie showing HEWL adsorption at the SiO_2 surface for the exemplar trajectory resulting in "between" final protein orientation on the surface. The surface atoms are shown by VdW spheres, the protein surface colored by name is shown as a ghost surface, the secondary structure is shown by a cartoon and anchor residues are indicated by licorice. Trajectory length is 100ns, water molecules are not shown. The most important residues are annotated at the initial and final stages of the trajectory.

pSiO$_2$V5.avi **–** a movie showing HEWL adsorption at the SiO_2 surface for the exemplar trajectory resulting in "side-on" final protein orientation on the surface. The coloring scheme is the same as for SiO_2V1.avi.

REFERENCES

(1) Phillips, J. C.; Braun, R.; Wang, W.; Gumbart, J.; Tajkhorshid, E.; Villa, E.; Chipot, Ch.; Skeel, R. D.; Kale, L.; Schulten K. Scalable Molecular Dynamics with NAMD. *J. Comput. Chem.* **2005**, 26, 1781-1802.

(2) Humphrey, W.; Dalke, A; Schulten, K. Visual Molecular Dynamics. *J. Molec. Graphics* **1996**, 14, 33-38.

(3) Sauter, C.; Otalora, F.; Gavira, J. A.; Vidal, O.; Giege, R.; Garcia-Ruiz, J. M. Structure of Tetragonal Hen Egg-White Lysozyme at 0.94 Å From Crystals Grown by the Counter-Diffusion Method. *Acta Crystallogr. D* **2001, *57***, 1119.

(4) Kubiak–Ossowska, K.; Burley, G.; Patwardhan, S. V.; Mulheran, P. A. Spontaneous Membrane-Translocating Peptide Adsorption at Silica Surfaces: A Molecular Dynamics Study. *J. Phys. Chem. B* **2013**, 117, 14666-14675.

(5) Kubiak-Ossowska, K.; Mulheran, P. A.; Nowak, W. Fibronectin Module $FN^{III}9$ Adsorption at Contrasting Solid Model Surfaces Studied by Atomistic Molecular Dynamics. *Phys. Chem. B,* **2014**, 118, 9900-9908.

(6) Patwardhan, S. V; Emami, F. S.; Berry, R. J.; Jones, S. E.; Naik, R. R.; Deschaume, O.; Heinz, H.; Perry, C. C. Chemistry of Aqueous Silica Nanoparticle Surfaces and the Mechanism of Selective Peptide Adsorption. *J. Am. Chem. Soc.*, **2012**, *134*, 6244-6256.

(7) Frenkel, D.; Smit, B. Understanding Molecular Simulation. Academic Press, London, 2002.

(8) Essmann, U.; Perera, L.; Berkowitz M. L.; Darden, T.; Lee, H.; Pederson, L. A Smooth Particle Mesh Ewald Method. *J. Chem. Phys.* **1995**, 103, 8577-8593.

(9) Kastenholz, M. A.; Hünenberger, P. H. Influience of Artificial Periodicity and Ionic Strenght in Molecular Dynamics Simulations of Charged Biomolecules Employing Lattice-Sum Methods, *J. Phys. Chem. B* **2004** 108, 774-788.

(10) Mulheran, P. A; Kubiak, K. Protein Adsorption Mechanisms on Solid Surfaces: Lysozyme-on-mica. *Mol. Sim.* **2009**, *35*, 561-566.

(11) Kubiak, K.; Mulheran, P. A. Molecular Dynamics Simulations of Hen Egg White Lysozyme Adsorption at a Charged Solid Surface. *J. Phys. Chem. B* **2009**, *113*, 12189-12200.

(12) Kubiak–Ossowska, K.; Mulheran, P. A. What Governs Protein Adsorption and Immobilization at a Charged solid Surface? *Langmuir* **2010**, *26*, 7690-7694.

(13) Kubiak–Ossowska, K.; Mulheran, P. A. Mechanism of Hen Egg White Lysozyme Adsorption on a Charged Solid Surface. *Langmuir* **2010**, *26*, 15954 – 15965.

(14) Kubiak–Ossowska, K.; Mulheran, P. A. Multiprotein Interactions during Surface Adsorption: a Molecular Dynamics Study of Lysozyme Aggregation at a Charged Solid Surface. *J. Phys. Chem. B* **2011**, *115*, 8891-8900.

(15) Kubiak-Ossowska, K.; Mulheran, P. A. Protein Diffusion and Long-Term Adsorption States at Charged Solid Surfaces. *Langmuir* **2012,** 28, 15577-15585.

(16) Larsericsdotter, H.; Oscarsson, S.; Bujis, J. Termodynamic Analysis of Lysozyme Adsorbed to Silica. J. Colloid. *Interface Sci.* **2004**, 276, 261-268.